

ICM11

Fatigue Strength of X45CrSi93 stainless steel applied as internal combustion engine valves

H. J. C. Voorwald^{a*}, R. C. Coisse, M. O. H. Cioffi

^a*Fatigue and Aeronautic Materials Research Group - DMT/FEG/UNESP – Univ Estadual Paulista, Av. Ariberto Pereira da Cunha, 333, CEP 12516-410 Guaratinguetá/SP, Brazil*

Abstract

Stainless steels are used to intake and exhaust valves production applied as internal combustion engines. In general valves are requested to support cyclic stresses applied due to opening and closing processes during the operation. The objective of this research is to study the influence on the axial fatigue strength of the resulting microstructure after heat treatment at the martensitic X45CrSi93 steel, combined with different surface treatments as hard chrome-plating, nitride and grinding. It was verified a significant increase on the fatigue strength of the martensitic steel after nitriding, compared with results from the chrome-plating specimens. A slight increase in the tensile strength was also noticed on nitrided parts as a consequence of a resistance increase due to nitrogen and carbon solid solution.

© 2011 Published by Elsevier Ltd. Selection and peer-review under responsibility of ICM11

Keywords: stainless steels; valves; nitride; fatigue

1. Introduction

Valves are components responsible for the opening of internal combustion engine cylinder in order to the moisture fuel-air to income during the intake stroke and for the exhaust of the burned combustion gases at the exhaust stroke as per showed in Figure 1a.

The applied stresses on valves during its service life are generated by the valve train dynamics, closing acceleration (due to the CAM shaft closing angle and spring force) and due to the combustion pressure. Diesel engines apply higher pressures at the valve face in comparison to Otto engines [1, 3].

The Figure 1b shows some typical combined stress distribution on an Otto intake valve fillet.



Fig. 1. a) Nomenclature of Engine Valves [3]. b) Stresses applied on an intake valve fillet area [4]

Regarding the Otto and Diesel engines, which present power and compression rate varying with time, during the combustion process put out gases and fuel vapor turn the environmental valves work extremely oxidant, specially because the operational temperature reach 550°C in the intake valves. The exhaust valves temperature is between 700°C and 800°C and, in some more severe cases, 900°C is achieved [1, 3], which justify the application of specific alloys

Fatigue failures can occur at the head area of valves causing radial cracks due to stresses generated by temperature gradients (Thermal Fatigue) or cordal crack (transversal cracks), near to seat face due to mechanical bending stresses.

At the keeper Groove area transversal cracks are also possible to occur due to the tensile stress combined to the geometric stress concentrator formed by the keeper groove radius. Corrosion is also a determinative factor in the fatigue failures [3].

Thermal failures can occur in intake valves due to the existence of hot spots inside the cylinder chamber, pre-ignition or gases leakages through the seat face.

2. Experimental Procedure

The X45CrSi93 Specimens have been prepared from hot rolled bars machined, quenched and tempered according to the following specifications: 30 minutes of austenitizing at 1040°C in an Ipsen T-6 furnace with 0.40% of carbon potential atmosphere and quenched in medium cooling rate oil; 60 minutes at 680°C in a continuous LWBU furnace and calm air cooled to reach 35 HRC/45 HRC, wich garatee the endurance and wear resistance, maintaining the ductility required to the impact resistance [3]. Specimen in Fig. 2 was performed according to ASTM E466 with constant radius between parallel sides [5].

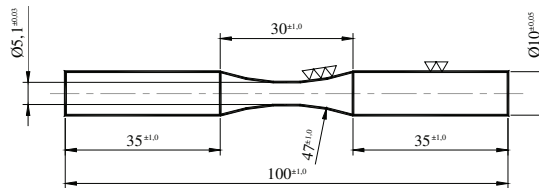


Figure 2 – Fatigue Specimen with dimensions in mm [5].

After heat treatment specimens were divided in two groups with different surface treatments:

- 1) Specimens nitrided in Sursulf process for 50 min at 530°C [6, 7];
- 2) The second group was chrome plated by electroplating in conventional equipment

The specimens were tested in tensile and axial fatigue using an INSTRON model 8801 equipment. A SEM Jeol model JSM – 5310, equipped with EDS was used to analyze the tensile and fatigue fractures.

3. Results

Specimens were identified as follows: 1BTC for chromed and 1BTN for nitrided parts. The average results for tensile strength and yield strength are represented in table 1.

Table 1 – Tensile test results

	Tensile Strength (MPa)	Yield Strength (MPa)
Not Plated	1062	897
Chrome-plated	1033	873
Nitrited	1148	970

Axial fatigue SxN curves are represented in Fig. 3. The fatigue limit is directly proportional to the mechanical strength [7] regarding to chemical composition, heat and thermochemical treatments. As hardness increases due to the chemical composition changes in the steel nitrided layer superficial mechanical resistance is higher, which is directly reflected by fatigue strength. To Shen et al. [8], this phenomenon is the consequence of increase in solid solution.

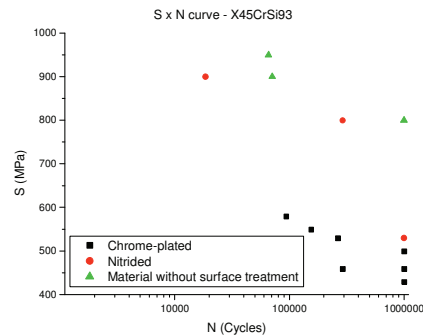


Figure 3 – Axial fatigue curve

The nitrided layer provides a blocking for surface movement of dislocations due to chemical structure change and by interstitial solid solution. The nitrogen in this region provides a dynamic aging process during the plastic deformation, which explains the yield strength and ultimate tensile strength difference by the nitrided specimens when compared to the chrome ones.

The chromium coating produce a tensile residual stress profile in the substrate associated to the fact that, during the chromium hydride decomposition, a mixture of chrome- α (CBC) and chrome- β (hexavalent) with density of 7,017 and 6,143, respectively, is formed generating an internal stresses [9], which are balanced by formation of a microcracked structure behaving as pre-existing cracks [10].

The surface cracks causes points of stress concentration, which change the local conditions of loading, because the stress in around of microcracks is greater than the average stress of nucleated surface crack with relatively low stresses [11]. The concentration of these forces causes the local fracture of the chromium layer leading to fracture.

Results of fatigue tests show an increase of about 50% in strength of nitrided specimens compared to the electroplated ones, associated to increase in mechanical strength regarding solid solution surface provided by the interstitial diffusion of nitrogen.

The found microstructure consists of tempered martensite with fine precipitated carbide throughout the matrix, as indicated in Figure 4.

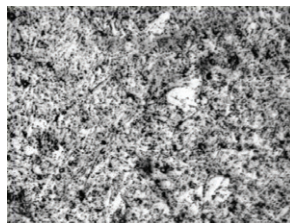


Figure 4 – Specimen core microstructure after quench and tempering – 1000x, Marble's.

3.1. Analysis of the nitrided material

For analysis of the nitrided region the hardness profiles, in order to determine the actual nitrogen diffusion depth, were initially raised. Results are shown in Figure 5.

Note that the surface hardness is between 622 and 848 HV_{0.05}, followed by a significant drop down to a minimum hardness associated to the matrix. The metallographic analysis of the nitrided layer has a surface layer of oxides, followed by a region of recrystallized grains and apparent decarburization.

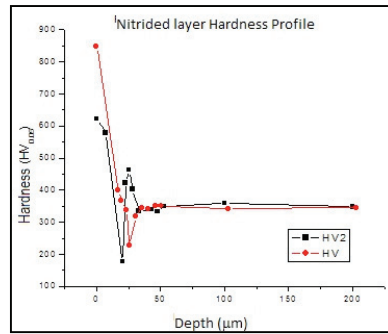


Figure 5 – Micro-hardness profile of the nitrided layer

Immediately below these grains, at the diffusion layer, it is possible to find some nitride precipitation at grain boundaries. The matrix microstructure is evidenced by approximately 60 μm from the surface. The compound layer, also known as white layer was not observed, due to loss of surface alloy verified by decarburization, which also caused the low hardness values even below the values found in the matrix core. In figures 6 a, b and c layers are shown.

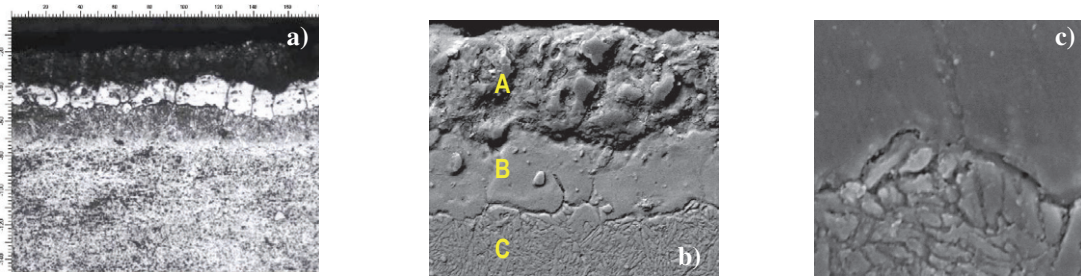


Figure 6 – a) Typical found Nitride layer microstructure, 400x, Nital 10%. (21BTN), b) Nitride layer microstructure formed below

the decarburized grains, 2,000x, Nital 10%. (21BTN), c) Microstructure of the interface between decarburization and diffusion layer 10,000x, Nital 10%. (21BTN)

The oxide layer, shown in figure 6 b as a region "A" has a large amount of silicon (8.6%), chromium (1.9%) and oxygen (3.4%), with relatively low iron content (86.1%), compared with other regions of the formed nitrided layer. In region B, the oxygen gives place to nitrogen, which shows concentration of 1.7% and silicon and chromium exhibit concentrations of 2.2% and 2.9% respectively and the iron content is 93.2%. Finally in region "C", regarded of diffusion layer, silicon and chromium concentrations present closer to the array, with 2.4% and 6.9% respectively. The iron, similarly presents concentrations closer to original composition of the alloy. The significant loss of alloying elements on layer "B" characterizes the decarburized region.

The figures 7a, b and c show darker regions, characterized by the lower amount of alloy elements with higher chemical weight [12]. The evidenced cracks were nucleated at the specimen surface, figure 7a; however, it was observed propagation in two entirely different ways. Even within the nitrided layer, it is possible to find more brittle fracture propagation. From the end of the intermediate diffusion layer a transgranular fatigue propagation is observed, in which the amount of nitrogen decreases significantly.

The fatigue crack propagation occurred through the oxide. In the decarburized layer, the fracture propagated primarily in two ways, with ductile and rough appearance in regions with higher concentration of alloying elements and brittle and smooth where these concentrations are lower and consequently the nitrogen contents are higher.

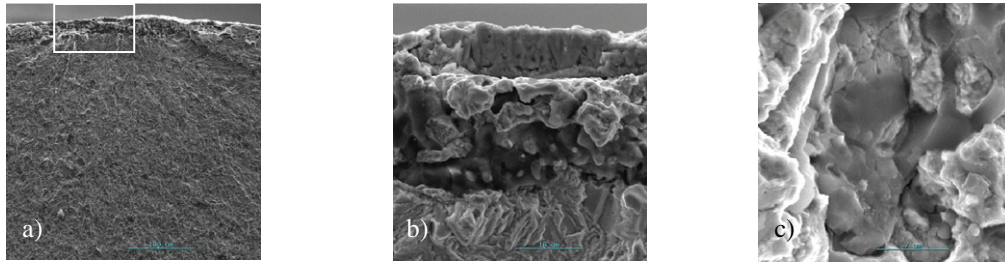


Figure 7 – a) Nucleation site and start of fatigue propagation; b) Detail of the fatigue crack nucleation site; c) Fracture surface in the decarburized region.

At the diffusion layer and at the specimen core the fracture propagation was typical transgranular up to the final rupture. It is possible, in figure 7b, to see the different fracture propagation between the regions with higher and lower nitrogen contents. The fatigue crack propagation below the surface layers is typically transgranular through the martensite laths is indicated in Figure 7c.

3.2. Analysis of the chrome-plated material

The chrome-plated presented along the surface an average hardness of 1050 HK measured from a load of 25g. The plate surface microcracks density was 327 fissures/mm², represented in Figure 8.

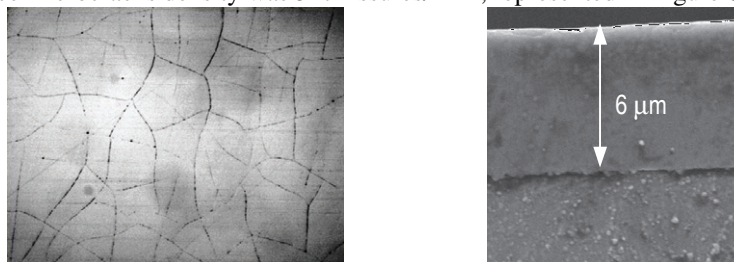


Figure 8 – a) Microcracks density at the surface. 200x not Etched; c) Chrome-plate metallographic, 10.000x, Nital 10%.

In the figure 8a it is also possible to see two layers of fissures on the studied plate. This fact occurs during the chrome-plate formation and can be considered as a cyclical phenomenon. After the deposition of certain chrome thickness, enough to raise the plate stress above the chromium resistance, the first cracks forms in order to relieve the stress. As the plating process continues the stress starts to grow again and new cracks are formed over the last one [8]. It was not evidenced so significant level of dealloying on the plated samples as found on the nitrided ones associated to the plated specimens needed to be polished and alkaline pickled as preparation for plating process. It was observed 6 μm chrome-plate as indicated in Figures 8b.

The fatigue fracture was nucleated at the specimen surface coincident to the chrome-plate cracks. The fracture at the chromium layer was brittle with signs of delamination (figures 9a), the propagation occurred through the chromium layer in different plans. These delaminations can be seen on the nucleation sites “A” and “B” in Figures 9 b and c.

According to Nascimento [10], the nucleation points on the chrome-plate and at the base material are lagged, mainly due to the difference between the stresses directions of each material and due to the fatigue crack propagation inside the chromium layer and at the interface with consequent plate delamination.

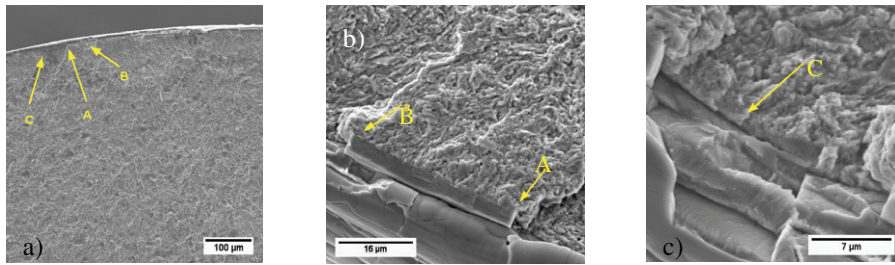


Figure 9 – a) Fracture initiation – 200x; b) Nucleation points “A” and “B” – 2.000x; c) Nucleation point “C” – 2.000x

4. Conclusion

The microstructural changes caused by nitrogen diffusion influenced the fatigue resistance. These changes in microstructure by solid solution equalize the detrimental effects of some defects caused by previous heat treatments; in this case quench and tempering as dealloying and decarburization.

The hard chrome-plating affects the mechanical steel behavior negatively, reducing its dynamic and quasi-static properties.

In all analyses cases in this study, the fatigue cracks initiated at the microcracks and propagated through the chrome layer causing some small plate delamination and nucleating several cracks on the specimens reducing fatigue life.

The tensile strength has also been affected by the chromium deposition and also by nitriding. The latter was responsible for a slight increase in this property.

Acknowledgements

This study was supported by Eaton Vehicle Division and by the Department of Materials and Technology of the Univ Estadual Paulista – UNESP.

References

- [1] Taylor, Charles Fayette – The Internal Combustion Engine in Theory and Practice, Combustion, Fuels, Materials, Design – Vol 2 - W. Hannover : The Massachusetts Institute of Technology, pag. 521-535 - 1977.
- [2] Larson, J. M., Jerkins, L. F., Narasimhan, S. L., Belmore, J. E. – Engine Valves – Design and Material Evolution – Journal of Engineering for Gas Turbines and Power – vol. 108/355-361 - 1987.
- [3] SAE J775 – Engine Poppet valve Information Report – SAE International, Surface Vehicle Information Report – Issued – 1961-06, revised 2004-11.
- [4] EATON - FEA Report – Report # 2009eng089 Eaton Italy, 2009
- [5] ASTM E466 - Standard Practice for Conducting Force Controlled Constant Amplitude Axial Fatigue Tests of Metallic Materials - E 466 – 96 (Reapproved 2002)
- [6] Centre Stéphanois de Recherches Mécaniques Hydromecanique ET Frottement – Sursulf nitriding in nonpolluting salt bath – Ed. Sc. Et Techniques, Paris.
- [7] Hertzberg, R. W. – Deformation and Fracture Mechanics of Engineering Materials – 4th Edition – New Jersey – John Wiley & Sons Inc. – 1996.
- [8] Y. N. Shen, H. H. Oh, D. N. Lee – Nitriding of steel in potassium nitrate salt bath. Scripta Materialia, 2005.
- [9] Nogueira, J. C. – Resistência Mecânica do Aço AMS-6414 (ABNT-4340), após desidrogenização em forno convencional, quando protegido com cromo duro e cádmio LHE (Low Hydrogen Embrittlement) – Master theses in Science at the mechanical Engineering, Physical and Chemical of Aerospace - ITA, São José dos Campos – 2003.
- [10] M. P. Nascimento, R. C. Souza, W. L. Pigatin, H. J. C. Voorwald – Effects of surface treatments on the fatigue strength of AISI 4340 aeronautical steel. International Journal of Fatigue, 23 (2001) 607–618.
- [11] J. K. Dennis; T. E. Such – Nickel and Chromium Plating. 1st Edition – England. Butterworth & Co Ltd, 1972
- [12] Colpaert, H – Metalografia dos produtos siderúrgicos comuns. 4a edição – São Paulo. Editora Blücher, 2008